

# Photovoltaic Characteristics and Dye Regeneration Kinetics in D149-Sensitized ZnO with Varied Dye Loading and Film Thickness

## Supporting Information

Ushula Mengesha Tefashe,<sup>[a]</sup> Melanie Rudolph,<sup>[b]</sup> Hidetoshi Miura,<sup>[c]</sup> Derck Schlettwein,<sup>[b]</sup>  
Gunther Wittstock<sup>\*[a]</sup>

[a] Ushula Mengesha Tefashe, Prof. Dr. Gunther Wittstock

Department of Pure and Applied Chemistry, Center of Interface Science, Faculty of  
Mathematics and Natural Sciences, Carl von Ossietzky University of Oldenburg,  
D-26111 Oldenburg, Germany

[b] Melanie Rudolph, Prof. Dr. Derck Schlettwein

Institute of Applied Physics, Justus Liebig University of Gießen, Heinrich-Buff-Ring 16,  
D-35392 Gießen, Germany

[c] Dr. Hidetoshi Miura

Chemicrea Co., Ltd., 2-1-6 Sengen, Tsukuba, Ibaraki 305-0047, Japan

\* To whom correspondence should be addressed

## SI1. Fitting of steady-state SECM approach curves with finite first order kinetics at the sample and diffusion controlled kinetics at the UME

Normalized heterogeneous rate constants  $\kappa$  have been extracted from experimental approach curves by fitting them to an analytical approximation of simulated data evaluated by Cornut and Lefrou.<sup>1</sup> The radius of the active part of the UME,  $r_T$ , the ratio  $RG$  of insulating sheath  $r_{\text{glass}}$  and  $r_T$ , and the point of closest approach  $d_0$  have been determined from independent experiments.  $RG$  was determined by optical microscopy;  $r_T$  and  $d_0$  were determined from approach curves to glass or D149/ZnO film in the dark and fitting them to theoretical curves proposed by Amphlett and Denuault.<sup>2</sup> The formula of Amphlett and Denuault given for  $RG = 10.2$ . Constants for other selected  $RG$  are also available.

$$I_T^{\text{cond}}(L) = 0.72627 + \frac{0.76651}{L} + 0.26015 \exp\left(\frac{-1.41332}{L}\right) \quad (\text{SI-1})$$

Normalized approach curves  $I_T$  vs.  $L$  have been calculated from each experimental approach curves  $i_T(z)$  using  $I_T = i_T/i_{T,\infty}$  and  $L = d/r_T$ . The analytical approximation of Cornut and Lefrou<sup>1</sup> was used for calculating a theoretical current  $I_T$  for each experimental, normalized distance  $L$ .

$$I_T(L, \kappa, RG) = I_T^{\text{cond}}\left(L + \frac{1}{\kappa}, RG\right) + \frac{I_T^{\text{ins}}(L, RG) - 1}{\left(1 + 2.47 RG^{0.31} L \kappa\right) \left(1 + L^{0.006 RG + 0.113} \kappa^{-0.0236 RG + 0.91}\right)} \quad (\text{SI-2})$$

with

$$I_T^{\text{cond}}\left(L + \frac{1}{\kappa}, RG\right) = \alpha(RG) + \frac{1}{2\beta(RG)\xi\left(L + \frac{1}{\kappa}\right)} + \left(1 - \alpha(RG) - \frac{1}{2\beta(RG)}\right)\xi\left(L + \frac{1}{\kappa}\right) \quad (\text{SI-3})$$

$$I_T^{\text{ins}}(L, RG) = \frac{\frac{2.08}{RG^{0.358}} \left( L - \frac{0.145}{RG} \right) + 1.585}{\frac{2.08}{RG^{0.358}} (L + 0.0023RG) + 1.57 + \frac{\ln RG}{L} + \frac{2}{\pi RG} \ln \left( 1 + \frac{\pi RG}{2L} \right)} \quad (\text{SI-4})$$

$$\alpha(RG) = \ln 2 + \ln 2 \left( 1 - \frac{2}{\pi} \arccos \left( \frac{1}{RG} \right) \right) - \ln 2 \left( 1 - \left( \frac{2}{\pi} \arccos \left( \frac{1}{RG} \right) \right)^2 \right) \quad (\text{SI-5})$$

$$\beta(RG) = 1 + 0.639 \left( 1 - \frac{2}{\pi} \arccos \left( \frac{1}{RG} \right) \right) - 0.186 \left( 1 - \left( \frac{2}{\pi} \arccos \left( \frac{1}{RG} \right) \right)^2 \right) \quad (\text{SI-6})$$

$$\xi \left( L + \frac{1}{\kappa} \right) = \frac{2}{\pi} \arctan \left( L + \frac{1}{\kappa} \right) \quad (\text{SI-7})$$

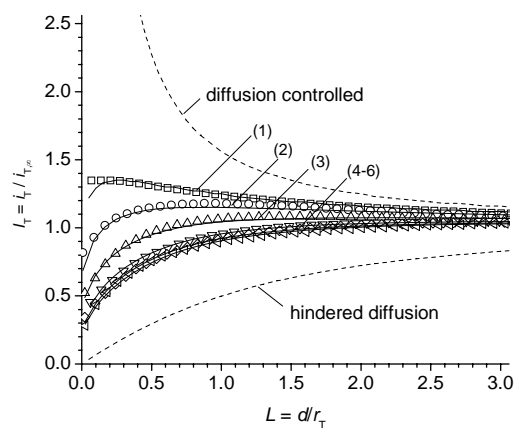
$$\kappa = \frac{k_{\text{eff}} r_T}{D} \quad (\text{SI-8})$$

$\kappa$ ,  $i_{T,\infty}$  and  $d_0$  (within reasonable range) were varied in order to fit the experimental approach curves. Heterogeneous rate constant  $k_{\text{eff}}$  was calculated from  $\kappa$ .

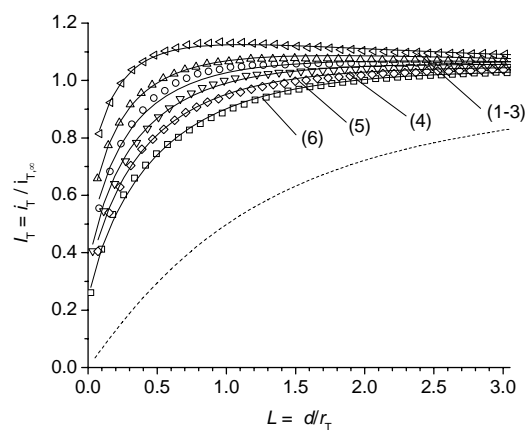
## SI2. SECM approach curves on D149/ZnO samples of $^{2.3}\text{S}_{2.6} - ^{0.4}\text{S}_{62.9}$

### a) SECM approach curves with varying $[\text{I}_3]^*$

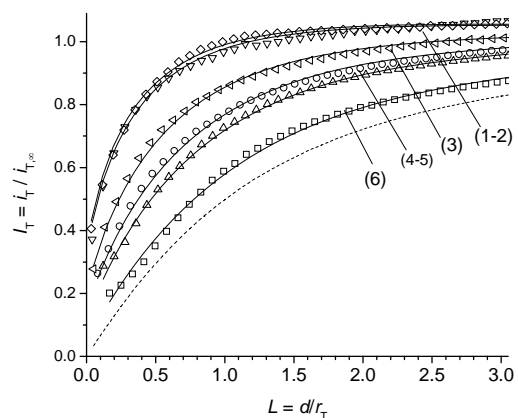
$^{2.3}\text{S}_{2.6}$



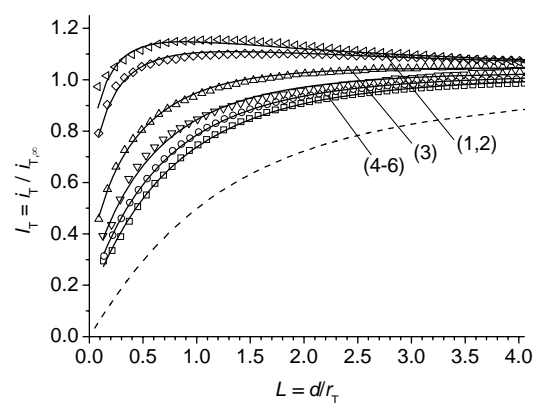
$^{3.3}\text{S}_{3.0}$



$^{1.8}\text{S}_{4.6}$



$^{1.8}\text{S}_{52.1}$



$^{0.4}\text{S}_{62.9}$

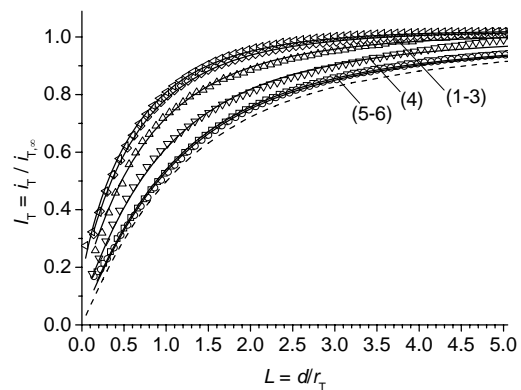
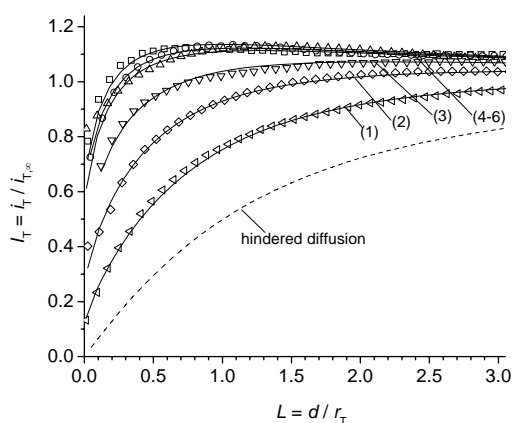


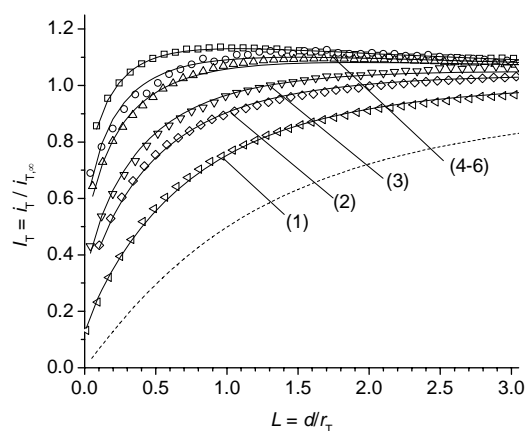
Figure SI-1. Normalized SECM approach curves obtained with Pt UME ( $r_T = 12.5 \mu\text{m}$ ) on D149/ZnO films of  $^{2.3}\text{S}_{2.6}$ ,  $^{3.3}\text{S}_{3.0}$ ,  $^{1.8}\text{S}_{4.6}$ ,  $^{1.8}\text{S}_{5.2,1}$  and  $^{0.4}\text{S}_{6.2,9}$  containing different  $[\text{I}_3^-]^*$ : (1) 0.057 mM, (2) 0.124 mM, (3) 0.248 mM, (4) 0.687 mM, (5) 1.24 mM and (6) 2.01 mM with  $E_T = -0.7 \text{ V}$  and  $J_{hv} = 9.1 \times 10^{-9} \text{ mol cm}^{-2} \text{ s}^{-1}$ . The summary of  $\kappa$  obtained from the best fits of experimental data (open symbols) to theoretical model (solid lines) were, respectively,  $^{2.3}\text{S}_{2.6}$ : (1) 1.18, (2) 0.75, (3) 0.44, (4) 0.28, (5) 0.24, (6) 0.22;  $^{3.3}\text{S}_{3.0}$ : (1) 0.66, (2) 0.50, (3) 0.41, (4) 0.25, (5) 0.19, (6) 0.12,  $^{1.8}\text{S}_{4.6}$ : (1) 0.40, (2) 0.28, (3) 0.18, (4) 0.09, (5) 0.06, (6) 0.02;  $^{1.8}\text{S}_{5.2,1}$ : (1) 0.74, (2) 0.60, (3) 0.42, (4) 0.28, (5) 0.11, (6) 0.08;  $^{0.4}\text{S}_{6.2,9}$  (1) 0.0195, (2) 0.0151, (3) 0.0089, (4) 0.0067, (5)  $9.03 \times 10^{-4}$ , (6)  $6.39 \times 10^{-4}$ . The top and bottom dashed curves in (a) represent responses limited by diffusion-controlled feedback and hindered diffusion, respectively.

**b) SECM approach curves with varying  $[\text{I}_3^-]^*$**

$^{2.3}\text{S}_{2.6}$



$^{3.3}\text{S}_{3.0}$



$^{1.8}\text{S}_{4.6}$

$^{1.8}\text{S}_{5.2,1}$

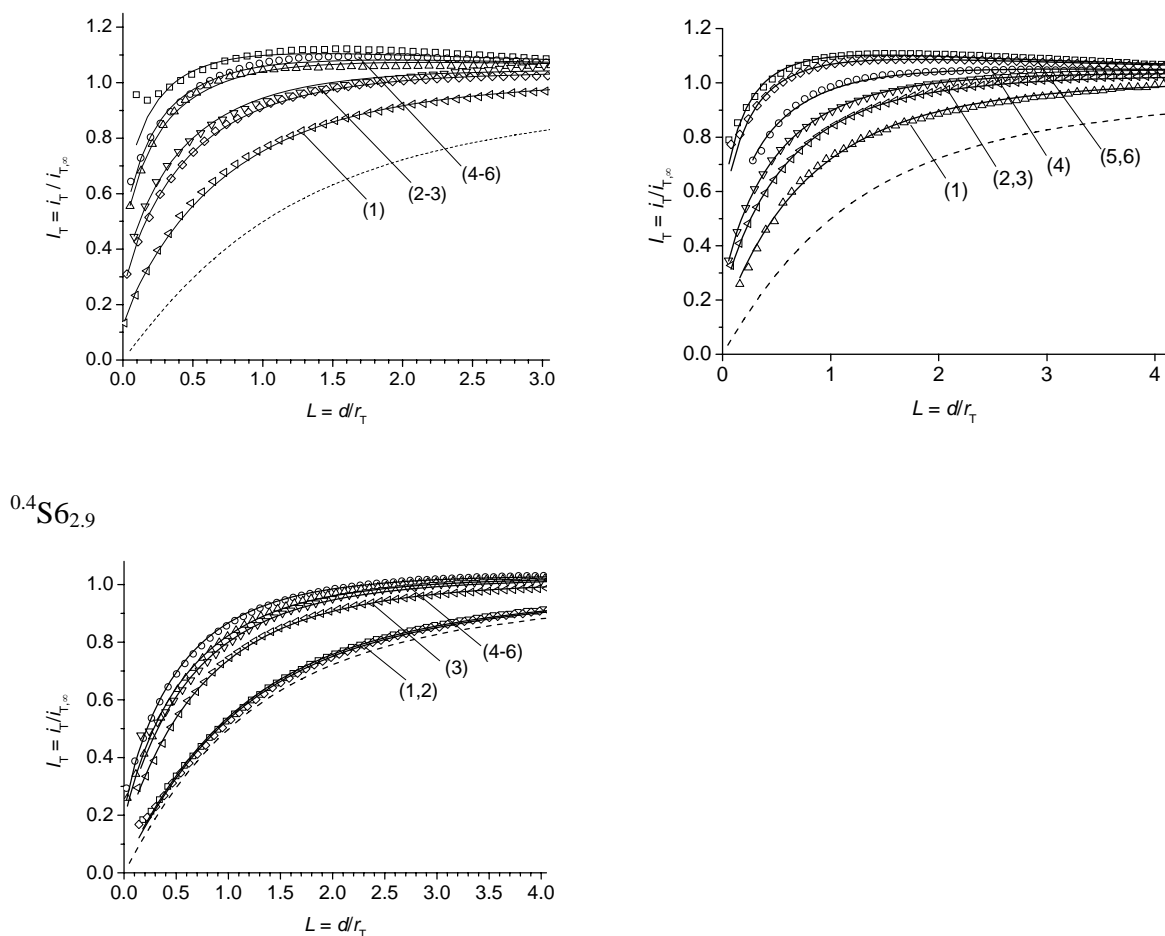


Figure SI-2. Normalized SECM approach curves obtained with Pt UME ( $r_T = 12.5 \mu\text{m}$ ) on D149/ZnO films of  $^{2.3}\text{S}_{2.6}$ ,  $^{3.3}\text{S}_{3.0}$ ,  $^{1.8}\text{S}_{4.6}$ ,  $^{1.8}\text{S}_{5.2.1}$  and  $^{0.4}\text{S}_{6.2.9}$  with  $[\text{I}_3^-]^* = 0.124 \text{ mM}$  with different  $J_{hv}$  ( $10^{-9} \text{ mol cm}^2 \text{ s}^{-1}$ ): (1) 0.982, (2) 1.70, (3) 4.50, (4) 9.10, (5) 15.1 and (6) 25.5,  $E_T = -0.7 \text{ V}$ . The summary of  $\kappa$  obtained from the best fits of experimental data (open symbols) to the theoretical model (solid lines) were, respectively,  $^{2.3}\text{S}_{2.6}$ : (1) 0.18, (2) 0.25, (3) 0.43, (4) 0.61, (5) 0.65, (6) 0.70;  $^{3.3}\text{S}_{3.0}$ : (1) 0.09, (2) 0.22, (3) 0.30, (4) 0.48, (5) 0.56, (6) 0.68,  $^{1.8}\text{S}_{4.6}$ : (1) 0.089, (2) 0.15, (3) 0.22, (4) 0.30, (5) 0.38, (6) 0.45;  $^{1.8}\text{S}_{5.2.1}$ : (1) 0.07, (2) 0.16, (3) 0.34, (4) 0.50, (5) 0.64, (6) 0.72;  $^{0.4}\text{S}_{6.2.9}$ : (1) 0.0006, (2) 0.0008, (3) 0.009, (4) 0.013, (5) 0.014, (6) 0.018. Dashed lines represent response controlled by hindered diffusion.

Table SI-1: Apparent heterogeneous first-order rate constants  $k_{\text{eff}}$  derived from normalized pseudo first order rate constants  $\kappa$  for the reduction of photoexcited D149 by  $\Gamma$  for D149-

sensitized ZnO photoelectrochemical electrodes of  $l$  and  $[D^0]$ . (a) For varying  $[I_3^-]^*$  at a fixed  $J_{hv} = 9.1 \times 10^{-9} \text{ mol cm}^{-2} \text{ s}^{-1}$  and (b) for varying  $J_{hv}$  at fixed  $[I_3^-]^* = 0.124 \text{ mM}$ . Other parameters  $D(I_3^-) = 1.37 \times 10^{-5} \text{ cm}^2 \text{ s}^{-1}$ ,  $r_T = 12.5 \text{ }\mu\text{m}$ ,  $RG = 10$ ,  $k_{\text{eff}} = \kappa D/r_T$ .

(a) For varying  $[I_3^-]^*$

$[I_3^-]^* / \text{mM}$	$k_{\text{eff}} / 10^{-3} \text{ cm s}^{-1}$					
	$^{1.3}\text{S}_{1.2}$	$^{2.3}\text{S}_{2.6}$	$^{3.3}\text{S}_{3.0}$	$^{1.8}\text{S}_{4.6}$	$^{1.8}\text{S}_{5.2.1}$	$^{0.4}\text{S}_{6.2.9}$
0.057	23.02	12.93	7.23	4.33	8.11	0.214
0.124	10.3	8.22	5.48	3.11	6.58	0.165
0.248	5.48	4.82	4.46	1.97	4.60	0.097
0.687	3.07	3.12	2.73	1.02	3.02	0.073
1.24	2.41	2.63	2.07	0.621	1.25	0.0099
2.01	2.26	2.41	1.32	0.212	0.93	0.007

(b) For varying LED intensity

$J_{hv} / 10^{-9} \text{ mol cm}^{-2} \text{ s}^{-1}$	$k_{\text{eff}} / 10^{-3} \text{ cm s}^{-1}$					
	$^{1.3}\text{S}_{1.2}$	$^{2.3}\text{S}_{2.6}$	$^{3.3}\text{S}_{3.0}$	$^{1.8}\text{S}_{4.6}$	$^{1.8}\text{S}_{5.2.1}$	$^{0.4}\text{S}_{6.2.9}$
25.5	9.96	7.67	7.45	4.93	7.85	0.198
15.1	9.10	7.12	6.14	4.16	6.98	0.157
9.10	8.10	6.74	5.22	3.31	5.44	0.138
4.50	4.77	4.71	3.30	2.39	3.71	0.093
1.70	2.78	2.74	2.41	1.64	1.70	0.0091
0.982	1.57	1.99	1.03	0.97	0.82	0.0071

### SI 3. Complete derivation of SECM model for dye regeneration

The following reaction mechanism for dye regeneration is widely accepted: We assumed similar molecular mechanism of dye regeneration in D149-sensitized ZnO and N179/TiO<sub>2</sub>. Therefore, using D149-sensitized ZnO electrode the model developed for steady state SECM experiments in the feedback mode.



Steady state for [D\*]

$$\frac{\partial [D^*]}{\partial t} = 0 = \phi_{hv} J_{hv} [D] - k_{inj} [D^*] \quad (SI-14)$$

$$\frac{[D]}{[D^*]} = \frac{k_{inj}}{\phi_{hv} J_{hv}} \quad (SI-15)$$

Steady state for [D⋯I]

$$\begin{aligned} \frac{\partial [D\cdots I]}{\partial t} = 0 &= k_1 [D^+] [I^-]_s - k_2 [D\cdots I] [I^-]_s \\ &= k_1 [D^+] - k_2 [D\cdots I] \end{aligned} \quad (SI-16)$$

$$\frac{[D\cdots I]}{[D^+]} = \frac{k_1}{k_2} \quad (SI-17)$$

Diffusion limited tip current ( $n = 2$ ) for reduction of one I<sub>3</sub><sup>-</sup>



$$i_{T,\text{lim}} = 8FD[I_3]^* r_T I_T(L) \quad (\text{SI-18})$$

Steady state for  $[D^+]$

$$\frac{\partial[D^+]}{\partial t} = 0 = k_{\text{inj}}[D^*] - k_1[D^*][I^-]_s \quad (\text{SI-19})$$

$$\frac{[D^+]}{[D^*]} = \frac{k_{\text{inj}}}{k_1[I^-]_s} \quad (\text{SI-20})$$

Combining (SI-17) with (SI-20)

$$\frac{[D \cdots I]}{[D^*]} = \frac{k_{\text{inj}}}{k_2[I^-]_s}$$

Mass balance for the total dye content

$$\begin{aligned} [D^0] &= [D] + [D^+] + [D^*] + [D \cdots I] \\ &= [D^*] \left( \frac{[D]}{[D^*]} + \frac{[D^+]}{[D^*]} + \frac{[D \cdots I]}{[D^*]} + 1 \right) \end{aligned} \quad (\text{SI-21})$$

Steady state expression for ratio of  $[D^0]$

$$[D^0] = [D^*] \left( \frac{k_{\text{inj}}}{\phi_{hv} J_{hv}} + \frac{k_{\text{inj}}}{k_1[I^-]_s} + \frac{k_{\text{inj}}}{k_2[I^-]_s} + 1 \right) \quad (\text{SI-22})$$

$$[D^*] = \frac{[D^0]}{\frac{k_{\text{inj}}}{\phi_{hv} J_{hv}} + \frac{k_{\text{inj}}}{k_1[I^-]_s} + \frac{k_{\text{inj}}}{k_2[I^-]_s} + 1} \quad (\text{SI-23})$$

The kinetic current  $i_k$  is expressed from the iodide concentration  $[I^-]_s$  at the surface of the dye-sensitized electrode, the volume concentration of the oxidized dye  $[D^+]$ . The current is generated over the thickness of the porous film  $l_{\text{porous}}$  and the area of the electrode  $A$ . The experimentally accessible dye loading  $\Gamma_D$  (total dye content per geometric area  $\Gamma_D = [D] l_{\text{porous}}$ ).

$$i_K = nFA(k_1 l_{\text{porous}} [D^+][I^-]_S) = nFA(k_1 \Gamma_{D^+} [I^-]_S) \quad (\text{SI-24})$$

Substitution of the bracketed term using the Bodenstein principle for the steady state experiment (SI-19) and introducing the dye loading yields  $k_{\text{inj}} \Gamma_{D^*} = k_1 \Gamma_{D^+} [I^-]_S$  ( $n = 1$ )

$$i_K = F A k_{\text{inj}} \Gamma_{D^*} \quad (\text{SI-25})$$

Substitute the expression for  $\Gamma_{D^*}$  from mass balance analogous to eq. SI-23.

$$i_K = F A k_{\text{inj}} \frac{\Gamma_{D^0}}{\frac{k_{\text{inj}}}{\phi_{hv} J_{hv}} + \frac{k_{\text{inj}}}{k_1 [I^-]_S} + \frac{k_{\text{inj}}}{k_2 [I^-]_S} + 1} \quad (\text{SI-26})$$

$$i_K = F A \Gamma_{D^0} \frac{\phi_{hv} J_{hv} k_1 k_2 [I^-]_S k_{\text{inj}}}{k_1 k_2 [I^-]_S k_{\text{inj}} + k_{\text{inj}} \phi_{hv} J_{hv} k_2 + k_{\text{inj}} \phi_{hv} J_{hv} k_1 + k_1 k_2 \phi_{hv} J_{hv} [I^-]_S} \quad (\text{SI-27})$$

$$\frac{1}{i_K} = \frac{1}{F A \Gamma_{D^0} \phi_{hv} J_{hv}} + \frac{1}{F A \Gamma_{D^0} k_1 [I^-]_S} + \frac{1}{F A \Gamma_{D^0} k_2 [I^-]_S} + \frac{1}{F A \Gamma_{D^0} k_{\text{inj}}} \quad (\text{SI-28})$$

Simplifying the expression for light absorption, electron injection and dye regeneration by

summarizing the steps using  $(k_{hv,eff})^{-1} = (k_{\text{inj}})^{-1} + (\phi_{hv} J_{hv})^{-1} \approx (\phi_{hv} J_{hv})^{-1}$  and

$$(k'_{ox})^{-1} = (k_1)^{-1} + (k_2)^{-1}$$

$$\frac{1}{i_K} = \frac{1}{F A \Gamma_{D^0} k_{hv,eff}} + \frac{1}{F A \Gamma_{D^0} k'_{ox} [I^-]_S} \quad (\text{SI-29})$$

The limiting substrate current would be reached if the iodide concentration is 3 time the triiodide concentration, i.e. all iodide formed at the tip is available to the sample without any dilution,  $[I^-]_S = 3[I_3^-]^*$

$$\frac{1}{i_{K,\text{lim}}} = \frac{1}{FA\Gamma_{D^{\circ}}k_{hv,\text{eff}}} + \frac{1}{3FA\Gamma_{D^{\circ}}k'_{\text{ox}}[I_3]^*} \quad (\text{SI-30})$$

Normalizing the limiting substrate by  $i_{T,\infty}$  yields  $I_{K,\text{lim}}$

$$I_{K,\text{lim}} = \frac{i_{K,\text{lim}}}{i_{T,\infty}} = \frac{i_{K,\text{lim}}}{4nFD[I_3]^*r_T}, \quad n = 2 \text{ at the tip for } I_3^-, A \approx \pi r_T^2 \quad (\text{SI-31})$$

$$\frac{1}{I_S} = \frac{i_{T,\infty}}{i_{K,\text{lim}}} + \frac{1}{I_{T,\text{cond}}} + \frac{1}{I_{\text{el,lim}}}, \quad \frac{1}{I_{\text{el,lim}}} \approx 0 \quad (\text{SI-32})$$

$$\begin{aligned} \frac{1}{I_S} &= \frac{1}{I_{T,\text{cond}}} + \frac{8FD[I_3]^*r_T}{F\pi r_T^2\Gamma_{D^{\circ}}\phi_{hv}J_{hv}} + \frac{8FD[I_3]^*r_T}{3F\pi r_T^2\Gamma_{D^{\circ}}k'_{\text{ox}}[I_3]^*} \\ &= \frac{1}{I_{T,\text{cond}}} + \frac{8D[I_3]^*}{\pi r_T\Gamma_{D^{\circ}}\phi_{hv}J_{hv}} + \frac{8D}{3\pi r_T\Gamma_{D^{\circ}}k'_{\text{ox}}} \end{aligned} \quad (\text{SI-33})$$

Comparison to uncomplicated first order process at the sample<sup>3</sup>

$$\frac{1}{I_S} = \frac{1}{I_{T,\text{cond}}} + \frac{4}{\pi} \frac{1}{\kappa}, \quad \kappa = k_{\text{eff}} \frac{r_T}{D} \quad (\text{SI-34})$$

$$\frac{1}{I_S} = \frac{1}{I_{T,\text{cond}}} + \frac{4D}{\pi r_T} \frac{1}{k_{\text{eff}}}$$

$$\frac{1}{I_S} = \frac{1}{I_{T,\text{cond}}} + \frac{4D}{\pi r_T} \left[ \frac{2[I_3]^*}{\Gamma_{D^{\circ}}\phi_{hv}J_{hv}} + \frac{2}{3\Gamma_{D^{\circ}}k'_{\text{ox}}} \right] \quad (\text{SI-35})$$

$$\frac{1}{k_{\text{eff}}} = \frac{2[I_3]^*}{\Gamma_{D^{\circ}}\phi_{hv}J_{hv}} + \frac{2}{3\Gamma_{D^{\circ}}k'_{\text{ox}}} \quad (\text{SI-36})$$

$$k_{\text{eff}} = \frac{3\Gamma_{D^{\circ}}\phi_{hv}J_{hv}k'_{\text{ox}}}{6k'_{\text{ox}}[I_3]^* + 2\phi_{hv}J_{hv}} \quad (\text{SI-37})$$

**SI 4. Dye regeneration kinetic model of reaction order 3/2 with respect  $[I^-]$ , Ref<sup>4</sup>**

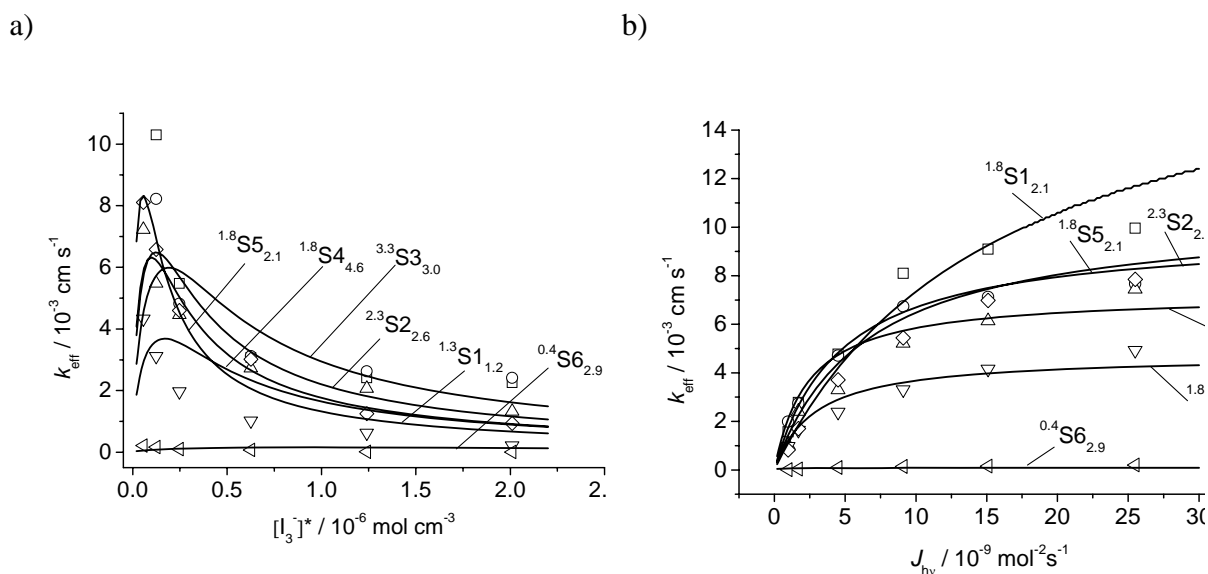


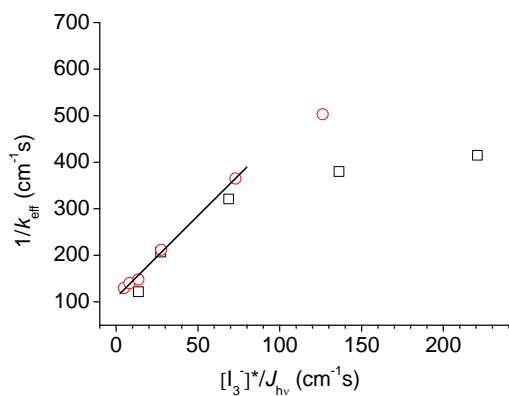
Figure SI-3. Plot of (a)  $k_{\text{eff}}$  vs.  $[I_3^-]^*$  and (b)  $k_{\text{eff}}$  vs.  $J_{h\nu}$  for six different D149-sensitized ZnO photoelectrodes with systematically varied thickness and dye loading. Symbols correspond to experimental  $k_{\text{eff}}$  and lines are theoretical fittings of the model described in Ref<sup>4</sup> [eq. 18]. The best fit of experimental and theoretical response of  $k_{\text{eff}}$  yielded a single value  $\phi_{h\nu}$  of  $2.29 \times 10^7 \text{ cm}^2 \text{ mol}^{-1}$  and varying  $k_{\text{ox}}$  by fitting the data for all electrodes in one set shown. The corresponding  $k_{\text{ox}}$  values are given in Table

Table SI-2: The  $k_{\text{ox}}$  obtained using the D149 regeneration reaction rate law of order 3/2.

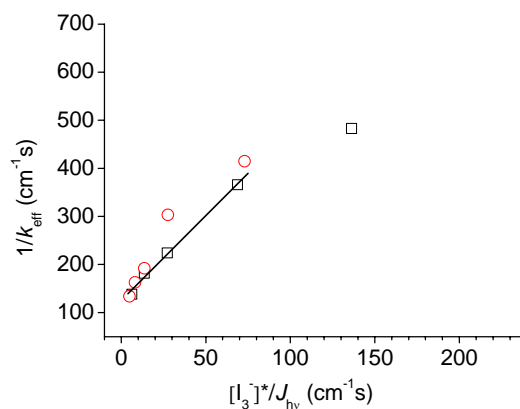
Sample	<sup>1.3</sup> S1 <sub>1.2</sub>	<sup>2.3</sup> S2 <sub>2.6</sub>	<sup>3.3</sup> S3 <sub>3.0</sub>	<sup>1.8</sup> S4 <sub>4.6</sub>	<sup>1.8</sup> S5 <sub>2.1</sub>	<sup>0.4</sup> S6 <sub>2.9</sub>
$k_{\text{ox}} / (\text{cm}^{9/2} \text{ mol}^{-3/2} \text{ s}^{-1})$	$1.59 \times 10^9$	$4.65 \times 10^8$	$2.40 \times 10^8$	$2.87 \times 10^8$	$6.45 \times 10^8$	$2.23 \times 10^7$

**SI 5: The  $k'_{ox}$  values obtained for D149/ZnO from the linear fit SECM kinetic model (eq. 12) in the manuscript.**

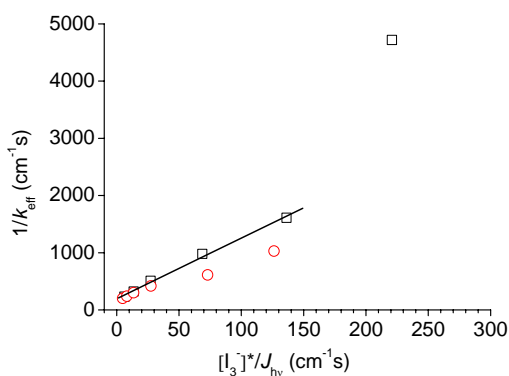
<sup>2.3</sup>S2<sub>2,6</sub>



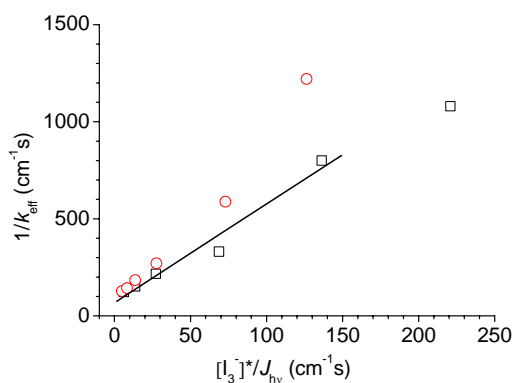
<sup>3.3</sup>S3<sub>3,0</sub>



<sup>1.8</sup>S4<sub>4,6</sub>



<sup>1.8</sup>S5<sub>2,1</sub>



<sup>0.4</sup>S6<sub>2,9</sub>

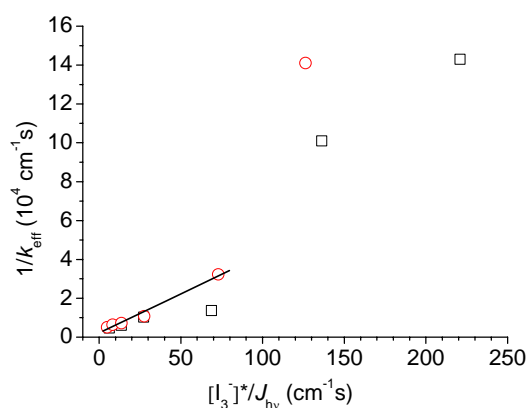


Figure SI 4. Plot of  $1/k_{eff}$  vs.  $[I_3^-]^*/J_{hv}$  for sample <sup>2.3</sup>S2<sub>2,6</sub> - <sup>0.4</sup>S6<sub>2,9</sub> showing a linear fit of the data at lower  $[I_3^-]^*/J_{hv}$  ratio.

Table SI-3: The  $k'_{\text{ox}}$  obtained from the linear fit in Figure SI 4 for kinetic model eq. (12) in manuscript

Sample	<sup>2.3</sup> S2 <sub>2.6</sub>	<sup>3.3</sup> S3 <sub>3.0</sub>	<sup>1.8</sup> S4 <sub>4.6</sub>	<sup>1.8</sup> S5 <sub>2.1</sub>	<sup>0.4</sup> S6 <sub>2.9</sub>
$k'_{\text{ox}} / (\text{mol}^{-1} \text{cm}^3 \text{s}^{-1})$	$2.64 \times 10^5$	$1.61 \times 10^5$	$1.89 \times 10^5$	$5.42 \times 10^5$	$7.56 \times 10^4$

#### References

1. R. Cornut and C. Lefrou, *J. Electroanal. Chem.*, 2008, **621**, 178-184.
2. J. L. Amphlett and G. Denuault, *J. Phys. Chem. B*, 1998, **102**, 9946-9951.
3. C. Wei, A. J. Bard and M. V. Mirkin, *J. Phys. Chem.*, 1995, **99**, 16033-16042.
4. Y. Shen, K. Nonomura, D. Schlettwein, C. Zhao and G. Wittstock, *Chem. Eur. J.*, 2006, **12**, 5832-5839.